CORRELATED MICROSCALE INVESTIGATIONS OF HYDROGEN ISOTOPES, WATER CONCENTRATIONS, AND REDOX STATE OF NOMINALLY ANHYDROUS MINERALS IN ICELANDIC BASALTS: IMPLICATIONS FOR MAGMATIC PROCESSES ON MARS. J. Davidson[1,2,*], M. Wadhwa[2], S. Sutton[3], R. L. Hervig[2], and T. Thordarson[4], [1]Buseck Center for Meteorite Studies, Arizona State University (ASU), Tempe, AZ 85287, USA. [2]School of Earth and Space Exploration, ASU, Tempe, AZ 85287, USA. [3]Department of the Geophysical Sciences and Center for Advanced Radiation Sources (CARS), University of Chicago, Chicago, IL 60637, USA. [4]University of Iceland, Sturlugata, Reykjavik, Iceland. *Email: jdavidson@asu.edu

Introduction: In order to understand the nature and origin of water in planetary materials, hydrogen isotope compositions and water abundances have been analyzed in extraterrestrial materials from Mars, the Moon, and asteroids (e.g., [1,2] and references therein). While these studies aid our understanding of the sources, abundance, and evolution of planetary water, with the exception of Apollo samples that were collected in the field by astronauts, they lack broader geologic context and the relationship between samples (if any) is not known. Meteorites, ejected from their host bodies by impacts and with different terrestrial residence times, have also been subjected to varying degrees of shock, cosmic ray exposure, and terrestrial contamination, which can affect their hydrogen isotope ratios and water concentrations [1,3]. To determine the primary magmatic signatures recorded in the meteorites, the effects of secondary processing must be understood and corrected. While future returned samples, such as those to be returned from Mars by the Mars Sample Return (MSR) program [4], will be essential to furthering these investigations, terrestrial analogs provide the opportunity to understand magmatic processes on planetary bodies in the absence of the effects of shock and cosmic ray exposure.

We focus on early-formed nominally anhydrous minerals (NAMs), such as olivine and pyroxene, which may be more reliable indicators of the hydrogen isotope compositions (expressed as δD) and H_2O concentrations (in parts per million by weight; ppm) of their parent magmas (e.g., [5,6]) than later formed minerals such as apatite (e.g., [1–3]). Combining δD–H_2O systematics with spatially correlated analyses of iron valence ($Fe^{3+}/\Sigma Fe$) can provide insights into petrogenetic processes (e.g., assimilation, dehydrogenation, and subsolidus diffusion) [7–12]. Our group previously reported combined H_2O–δD–$Fe^{3+}/\Sigma Fe$ systematics of NAMs in terrestrial kaersutite amphiboles [7] and pyroxenes from Mars [9–11] and the Moon [12], demonstrating the validity of this approach.

Here we report the combined H_2O–δD–$Fe^{3+}/\Sigma Fe$ systematics of NAMs from Icelandic basalts. The goal of this work is to aid understanding of the variability in hydrogen isotope compositions and redox within and among martian meteorites.

Sample Collection: Samples were collected from seven Icelandic localities, including Litla-Sandfell and Kverkfjöll, in August and September 2017. At Litla-Sandfell, a 60 cm thick, heavily vesiculated, pillow lava lobe was sampled every ~12 cm (top to base: 09 to 13). At Kverkfjöll, a 3×2 m pillow lava was sampled vertically three times (top to core: 3A to 3C). These localities were chosen as they may show evidence for degassing or exhibit fractional crystallization behavior.

Analytical Methods: Chips (~1g) were removed from each larger sample with a hammer and crushed with an agate pestle and mortar. NAMs (predominantly olivine) were then hand-picked under a binocular microscope. Individual mineral grains were hand-polished without the use of water, oil, or glue by the method of [5]. A total of 34 grains from Litla-Sandfell and 10 grains from Kverkfjöll were co-mounted with terrestrial standards in indium metal in a single Al disc. Approximate relative locations of grains in pillow lava lobes are shown in Fig. 1. Quantitative compositional analyses and high-resolution secondary and backscattered electron imaging were undertaken on ASU's JEOL JXA-8530F electron probe microanalyzer (15 kV, 15 nA).

Secondary Ion Mass Spectrometry (SIMS): Measurements of H isotope compositions and H_2O concentrations of NAMs were performed on the Cameca IMS-6f SIMS at ASU using analytical protocols described in more detail in [3,6]. Eight Kverkfjöll grains (six olivine, two pyroxene) and 16 Litla-Sandfell olivine grains and one olivine-hosted melt inclusion were analyzed. We corrected for the background H_2O concentrations during each analytical session (6 and 8 ppm H_2O), determined by analyses of nominally anhydrous San Carlos olivine and dehydrated PMR53 pyroxene (method of [13]).

X-ray Absorption Near-Edge Structure (XANES): The Fe K XANES spectra were collected on spots adjacent to the SIMS pits on each of one pyroxene and six olivine grains from Kverkfjöll using station 13-ID-E at the GSECARS X-ray microprobe at the Advanced Photon Source at Argonne National Lab, following the method of [7]. Litla-Sandfell samples will be analyzed at a later date. For each analysis spot (~1 μm diameter), spectra were collected at four different orientations, accomplished by rotating the sample mount through 90 degree increments, and were merged to form a single spectrum. The Fe valence was determined using the "Lasso" (least absolute shrinkage and selection operator) method described in [14]. Average Fe valences are

reported as "2 + (Fe^{3+}/ΣFe)"; precision is estimated to be ± 0.008 (1σ) based on the average intragrain standard deviation for homogeneous grains.

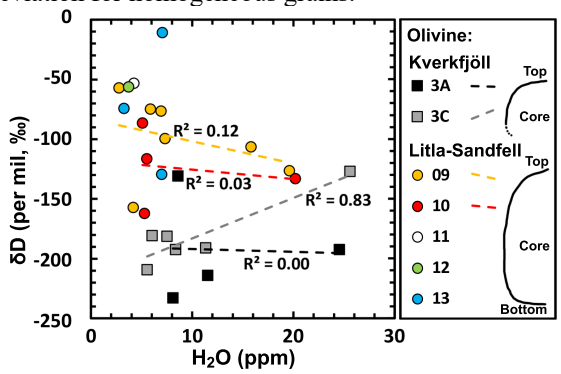

Fig. 1: *Water concentrations (H_2O in ppm) versus H isotope compositions (δD in per mil) for olivines from Litla-Sandfell and Kverkfjöll. Positions in lobes are shown to the right.*

Results: Olivines from Litla-Sandfell samples have light H isotope compositions (δD = –162 ± 94 ‰ to –11 ± 110 ‰; 2σ errors) and low H_2O contents (3 ± 1 ppm to 20 ± 4 ppm) (Fig. 1); there was no discernable statistically significant difference between olivines sampled at different depths within the pillow lava (09 = top, 13 = bottom). One melt inclusion analyzed had a higher water concentration (H_2O = 1610 ± 320 ppm) and similar H isotope composition (δD = –142 ± 16 ‰) compared to the olivines.

Olivines from Kverkfjöll samples have light H isotope compositions (δD = –233 ± 72 ‰ to –127 ± 76 ‰) and low H_2O contents (6 ± 1 ppm to 26 ± 5 ppm); there was no discernable difference between olivines sampled at the pillow lava's surface (3A) and core (3C) (Fig. 1). While Kverkfjöll pyroxenes have comparable H isotope compositions (δD = –164 ± 17 ‰ and –142 ± 35 ‰), they have much higher water concentrations (389 ± 78 ppm and 146 ± 29 ppm, respectively) than those of olivine. The Fe valences of olivines (Fe^{3+}/ΣFe, 1σ errors) range from 2.014 ± 0.008 to 2.026 ± 0.008 (Fig. 2), and have an average of 2.022 ± 0.005 for 3A and 2.016 ± 0.003 for 3C (2.018 ± 0.005 overall). A single pyroxene analyzed has a value of 2.225 ± 0.008.

Discussion: Olivines from Kverkfjöll are generally isotopically lighter than those from Litla-Sandfell while both suites cover a comparable range of water concentrations (Fig. 1). There is no apparent correlation between H isotope compositions and water concentrations in Litla-Sandfell olivines, though there may be a positive correlation in olivines from the core of the Kverkfjöll lobe (3C: coefficient of determination, R^2 = 0.83), which could indicate H_2O release (i.e., dehydration [8]). However, this is not supported by Fe redox data for 3C, which shows no correlation with either H isotope compositions or water concentrations (Fig. 2). Furthermore, Fe redox states for 3A (pillow surface) and 3C (core) agree within error.

The general lack of correlation may be due to the low water concentrations analyzed making it difficult to discern a statistically significant trend. However, we previously identified degassing trends in pyroxenes from Lafayette (martian nakhlite) with <30 ppm water concentrations [6,9], similar to those seen here.

There may be a weak correlation (R^2 = 0.68) between water concentration and Fe valence state in olivines from Kverkfjöll 3A (pillow surface) (Fig. 2b), which would indicate H_2 release (i.e., dehydrogenation [8]). However, Fe redox evidence for hydrogen release has typically been observed in pillow interiors during cooling and crystallization and not at the surface [15].

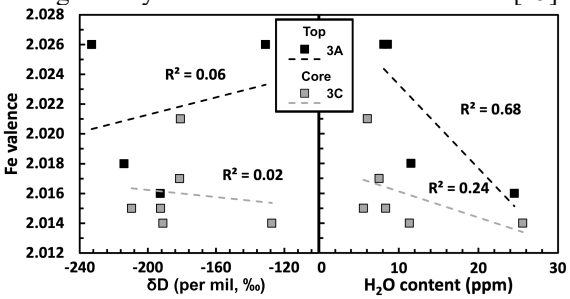

Fig. 2: *Fe valences of olivines from Kverkfjöll 3A (top) and 3C (core) versus (a) H isotope compositions (δD in per mil), and (b) water concentrations (H_2O in ppm).*

Summary: While H_2O–δD of olivine from the Kverkfjöll pillow lava core (3C) may record evidence for degassing (though this is not reflected in Fe redox data), there is generally no correlation between H_2O–δD in olivine from Litla-Sandfell, regardless of position in the pillow lava lobe. Future work will extend Fe^{3+}/ΣFe analyses to Litla-Sandfell olivines, more pyroxene grains from both suites, and another suite of Icelandic basalts. The higher water concentrations present in pyroxenes will likely make correlations between H_2O–δD–Fe^{3+}/ΣFe (if any) more apparent (e.g., [9,10]).

Acknowledgments: This work was supported by NASA NNX16AT37G (M.W.), NSF EAR-1352996 (ASU SIMS) and NSF EAR-1634415 (GSECARS).

References: [1] Hallis L. et al. (2017) *PTRSA*, *375*, 20150390. [2] Lin Y. and van Westrenen W. (2019) *NSR, 6,* 1247–1254. [3] Davidson J. et al. (2020) *EPSL, 552,* 116597. [4] Beaty D. W. et al. (2019) *MAPS, 54,* S3–S152. [5] Peslier A. H. et al. (2019) *GCA*, *266*, 382–415. [6] Davidson J. et al. (2020) *LPS LI*, #1660. [7] Wadhwa M. et al. (2019) *MetSoc*, #6473. [8] Demény A. et al. (2006) *RCMS, 20,* 919–925. [9] Davidson J. et al. (2021) *LPS LII*, #2103. [10] Davidson J. et al. (2022) *LPS LIII*, #1546. [11] Davidson J. et al. (2022) *MetSoc*, #6109. [12] Wadhwa M. et al. (2022) *MetSoc*, #6501. [13] Mosenfelder J. L. et al. (2011) *AM*, *96*, 1725. [14] Dyar M. D. et al. (2016) *AM*, *101*, 1171–1189. [15] Christie D. M. et al. (1986) *EPSL, 79,* 397–411.